VOL. 20, NO. 2-2, 2021, 30-35
www.elektrika.utm.my
ISSN 0128-4428

ELEKTRIKA
Journal of Electrical Engineering

Numerical Simulations for Two Way Shape-Memory-Alloy MEMS 3D Tunable Inductors

Soffia Tasneem Ahmad Fua'ad and **Mohamed Sultan Mohamed Ali***

School of Electrical Engineering, Universiti Teknologi Malaysia, 81310 UTM Johor Bahru, Johor, Malaysia.

*Corresponding author: sultan_ali@fke.utm.my

Abstract: This paper presents numerical simulations for microelectromechanical systems (MEMS) tunable 3D inductor using two-way shape-memory-alloy (SMA). MEMS inductors are significant to develop the small scale, lightweight and high-performance wireless communications technologies. The inductance value often varied depending on its application. Hence in this work, a 3D tunable inductor is developed using two-way SMA actuation. A numerical simulation is performed by using COMSOL Multiphysics software to evaluate the temperature of the SMA inductor during Joule heating and the inductance values based on its actuation heights. The results of the numerical simulations show that when a 0.4 A DC current is supplied, the temperature at the spiral coil of the 3D tunable inductor reaches 67.86 °C. Meanwhile the inductance value of the 3D tunable inductor is lower when the height of the actuation is increased. When the height of the 3D tunable inductor is at 6mm and 3.6mm, the inductance value is 0.97nH to 1.56nH respectively. It is expected that the results if work would encourage developments of 3D tunable inductors in wireless displacement sensor.

Keywords: Inductors, MEMS, SMA.

Article History: received 25 May 2021; accepted 12 June 2021; published 15 September 2021.

1. INTRODUCTION

MEMS inductors have begun to receive more attentions due to their suitability for mass production using the standard complementary metal oxide semiconductor (CMOS) manufacturing technology [1]. The performance of the inductors depends on its figure of merits which are the inductance value, quality factor (Q-factor), self-resonance frequency (SRF) and tuning range. However, according to Pisani *et al* [2], this CMOS technology has disadvantages due to its low thin-film inductors of 1-2 µm in thickness are not enough to achieve high-Q inductors and standard CMOS fabrication technology doesn't support thick metallization process [3]. Besides, silicon is the main substrate used in CMOS devices and it has relatively low resistivity that also contribute to the performance degradation. This has been a major cause of losses for passive components that are fabricated over it, especially for micro inductors. The losses are in the form of eddy currents flowing in circles within the substrate, and parasitic capacitance formed between the substrate and inductor's windings. Thus, CMOS inductors have continued to suffer from low-Q factors [4], degrading the performance of many RF devices.

To improve the performance of CMOS-based inductors, variety of techniques have been applied and evaluated. Post-CMOS electroplating were used to provide tens of microns of coil thickness, which are not feasible with standalone CMOS fabrication. Other techniques to reduce substrate losses include: the use of high-resistivity substrate [3], the use of low-K dielectric between the substrate and the inductor [5], the use of patterned ground shield above the substrate [6], etching the substrate from underneath the inductor [7], and even building multilayer inductors [8, 9].

On the other hand, MEMS tunable inductors offered a better performance, due to its flexibility and the many advanced machining techniques that MEMS fabrication provides compare to CMOS inductors that are mostly confined to planar spiral types. The most attracted MEMS inductors designs are those of 3D geometries such as solenoid inductors [10, 11], 3D inductors [12-14], flexible inductors [15], out-of-plane inductors [16], and vertical inductors [17]. These topologies show great performances, but they require complicated fabrication processes.

To reduce the fabrication complexity of the tunable inductor, shape-memory-alloys (SMA) is utilized. The SMA have different shape memory effect (SME) which are one-way memory effect and two-way memory effect. One-way SME involves the memorization of the SMA predetermined shape to which they deform once exposed to a stimulus such as heat. Two-way SME is the effect that the material will memorize two different shapes; in austenite and martensite states To have two-way SME training methods plays an important role in two-way actuations [18]. This approach has so far been used in many applications to provide mechanism to many SMA actuators such as fabrications of catheter, cardiovascular stent and micro actuators of various shapes [19, 20]. Furthermore, the electrical properties of SMA allows it to

be joule-heated by means of passing electrical current to raise its internal temperature to control the actuation heights.

In this paper, the 3D tunable inductor's Joule heating and tuning range is evaluated. The numerical simulations are perfected by using COMSOL Multiphysics software. A design and fabrication processes proposal of out of plane tunable inductor is presented.

2. Design and Working Principle of Tunable Inductor

In this section, design of tunable inductor with specific dimensions is proposed. In addition, the working principle of the tunable inductor is explained further.

2.1 Design of Tunable Inductor

The inductance value for spiral inductor is calculated by approximating the sides of the spiral with symmetrical current sheets of equal current densities, another simple and accurate expression for the inductance of a planar spiral can be obtained [21]. For example, in this case of the circular coil as shown in Figure 1, we obtain 4 identical current sheets. On opposite sides, the existing sheets are parallel. The calculation of the inductance is now reduced to measuring the self-inductance of one sheet and the mutual inductance between opposite current sheets, thanks to symmetry and the fact that the sheets have zero mutual inductance.

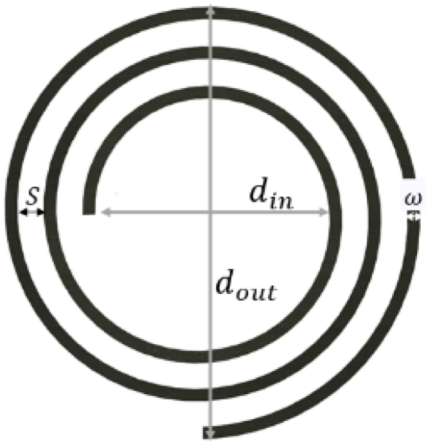

Figure 1. Inductance value calculation for spiral coil

These self and mutual inductances are evaluated using the concepts of geometric mean distance, arithmetic mean distance, and arithmetic mean square distance. Thus the resulting expression for spiral coil inductor L_{gmd} is presented by [21],

$$L_{gmd} = \frac{\mu n^2 d_{avg} c_1}{2} \left(\ln\left(\frac{c_2}{\rho}\right) + c_3\rho + c_4\rho^2\right) \qquad (1)$$

where μ is the magnetic permeability of the material, n is the number of turns, d_{avg} is the average diameter of the spiral coil calculated by $0.5(d_{out} + d_{in})$. The values of coefficient $c_1, c_2, c_3,$ and c_4 are 1.00. 2.46, 0.00, and 0.20 respectively, and layout dependent, ρ is fill ratio calculated by $(d_{out} - d_{in})./(d_{out} + d_{in})$.

As a proof of concept for tunable inductor, it has five circular spiral turns with the coil width of 0.4 mm and separation of 0.2 mm respectively. The diameter of the spiral coil is 7.2 mm as illustrated in Figure 2. The SMA inductor with mentioned dimensions above is designed in Solidwork software. By using formula (1), the theoretical value of the inductance is 1.36 nH.

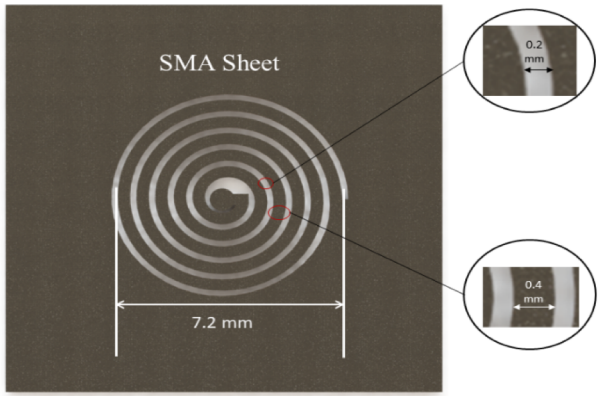

Figure 2. Solidwork design of 2D spiral coil inductor

2.2 Working Principle of Tunable Inductor

Nitinol is a metal alloy of nickel and titanium with its unique mechanical properties such as superelasticity, ductility and thermal memory [22]. The SMA has two distinct state which are martensite state and austenite state controlled by temperature and internal stresses. At lower temperature, it is called martensite state and at higher temperature it is called austenite state. Nitinol shape can be altered during rapid cooling from austenite state to martensite state. To adopt 3D out-of-plane actuation that manipulate the separation of the coils to alter the inductance value, the SMA needed to undergo training to memorize two out-of-plane states; in martensite and austenite state as shown in Figure 3.

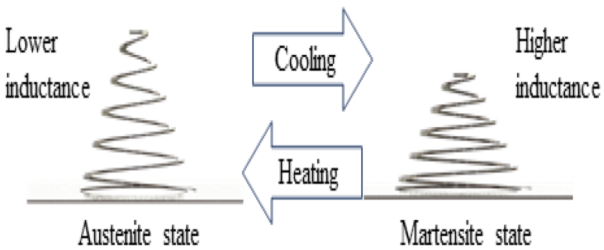

Figure 3. At austenite state and martensite state, the inductance value differs.

To achieve both austenite and martensite state, the 2D spiral inductor will undergo two-way shape memory training. A mold that consists of inner mold and outer mold is proposed as shown in Figure 4 (a), to shape 2D spiral inductor to 3D out-of-plane spiral inductor, this process

also known as one-way shape-memory setting. To secure the 3D configuration of the spiral coil, the spiral coil is loaded in the molds, Figure 4 (a), and go through heat treatment process with ~400 °C [23] using an oven and then the whole thing will be dipped in cold water for rapid cooling. These procedures will complete the one-way shape-memory setting and expected in memorization of austenite shape as shown in Figure 4 (b).

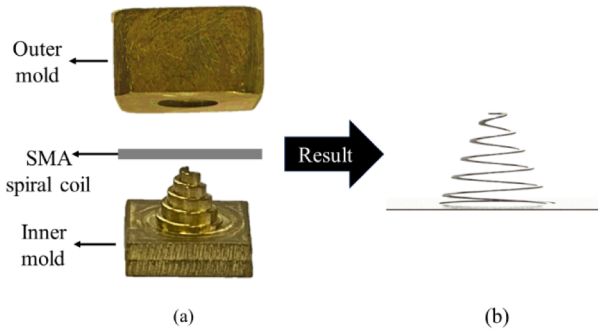

Figure 4. Training process; (a) one-way shape-memory setting, (b) one-way trained SMA spiral coil

To create a 3D tunable inductor, the inductor must memorize another shape in its martensite state thus it involves a second shape-memory setting known as two-way shape-memory setting. By referring *Luo et al*. [18], pseudoelastic cycle procedure have to be done where the spiral coil is introduced at a temperature, 300 °C [24]. At this temperature the SMA spiral coil will exhibit pseudoelasticity behavior. To complete a pseudoelastic cycle, a load is placed on top of the 3D spiral SMA, Figure 5 (a), and heated to 300 °C. Afterwards, SMA spiral coil will be cooled to room temperature in loaded condition and then it is unloaded completely as shown in Figure 5 (b). A total of 40 pseudoelastic cycles are needed to achieve a noticeable two-way shape-memory effect.

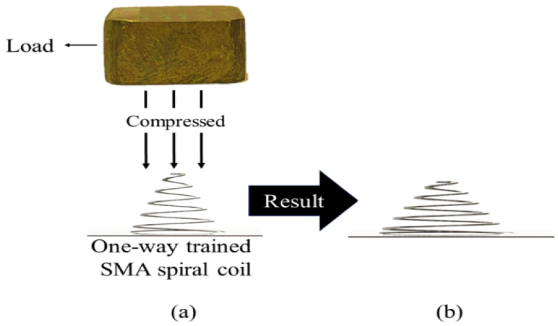

Figure 5. Training process; (a) two-way shape-memory setting, (b) two-way trained SMA spiral coil.

3.COMSOL MULTIPHYSICS NUMERICAL SIMULATION

In this section, the results of COMSOL Multiphysics numerical simulations for both Joule heating and inductor tuning range is presented and discussed.

3.1 Joule Heating Module

In the Joule heating simulations, 0.1 A, 0.2 A, 0.3 A, 0.4 A and 0.5 A DC current is supplied, the temperature varies. As we can see in Figure 6, the current supplied is directly proportional to the temperature of the 3D tunable inductor. It is stated by [24] at 65 °C the peak actuation of the 3D tunable inductor will takes place. Hence, in Figure 7 and Figure 8, when 0.4 A DC current is introduced, the simulation result shows that the maximum temperature is 67.86 °C and is heated evenly from the terminal to the ground of the 3D tunable inductor.

Apparently as illustrated in Figure 7 (a), the base and the spiral coil of the 3D tunable inductor have different temperature where the base remains at room temperature while the spiral coil is being heated. This is due to the base have lower resistance than the spiral coil. In Figure 7 (b), the circular shape is asymmetry between each coil causes them to have different resistance value consequently

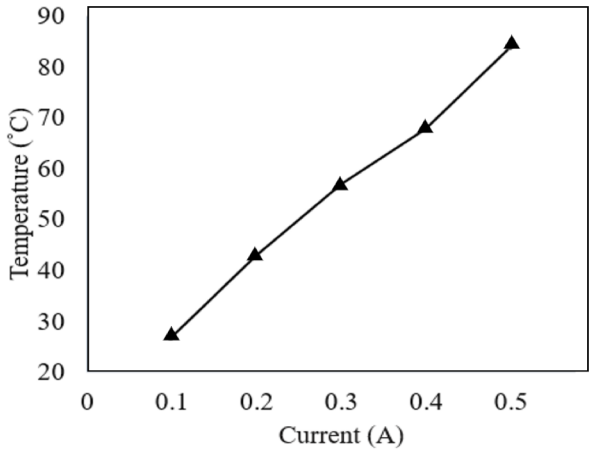

Figure 6. Current (A) *vs* temperature (°C)

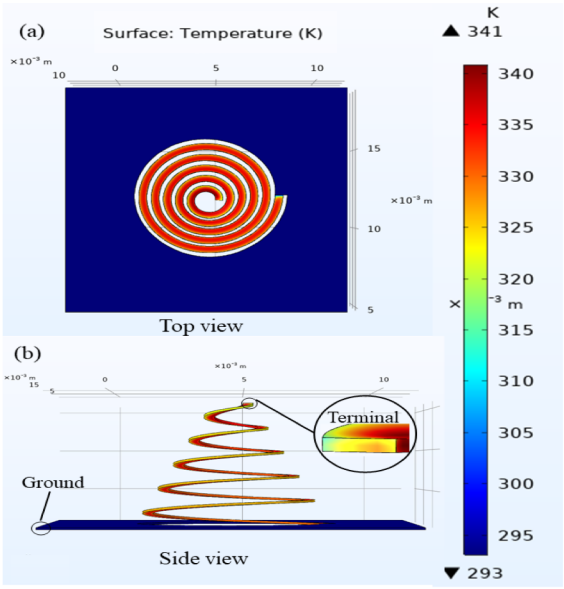

Figure 7. Joule heating module simulation. (a) Top view (b) Side view

causes the temperature in the spiral coil of the 3D tunable inductor is unevenly distributed.

3.2 Inductor Tuning Range

Magnetic and electric fields module is simulated to determine the inductance value based on the distance the coils. The simulation results show that the spiral coils with closer separation has higher inductance value and vice versa.

In Figure 8(a), (b), (c), and (d), shows the values of inductance values and their heights. When the heights of the 3D tunable inductor are at 3.6mm and 6mm, the inductance values are 1.56 nH and 0.97 nH respectively. It is confirmed that the inductance value is higher when the separation between coils is closer to each other.

At austenite state, a 0.4 A DC current is applied causing the 3D tunable inductor to actuate at its maximum peak, 6mm causes a noticeable separation between the coils. This has led to more Eddy current loss, hence reduce the inductance values. Meanwhile at martensite state, the 3D tunable inductor is at room temperature the height remains at 3.6mm. The separation of the coils is closer to each other resulting in less Eddy current loss, consequently, have higher inductance values. A total of 60.8% tuning range is calculated for both maximum and minimum inductance value shows that the SMA spiral coil has high tuning range.

However, at 4.8mm and 5.4 mm heights of the 3D tunable inductor, there is insignificant changes in the inductance value which are 1.28 nH and 1.23 nH. There is only a total of 4% tuning range. This explains as the temperature rises evenly in the coil, all segments contribute equally to provide maximum vertical actuation accompanying to worthless Eddy current loss. Owing to the unidirectional actuation from the top terminal of the coil to the bottom ground of the coil, the inductance value varies insignificantly during the transition from minimum to maximum actuation. Therefore, the height of the 3D tunable is inversely proportional to the inductance value as illustrated in Figure 9.

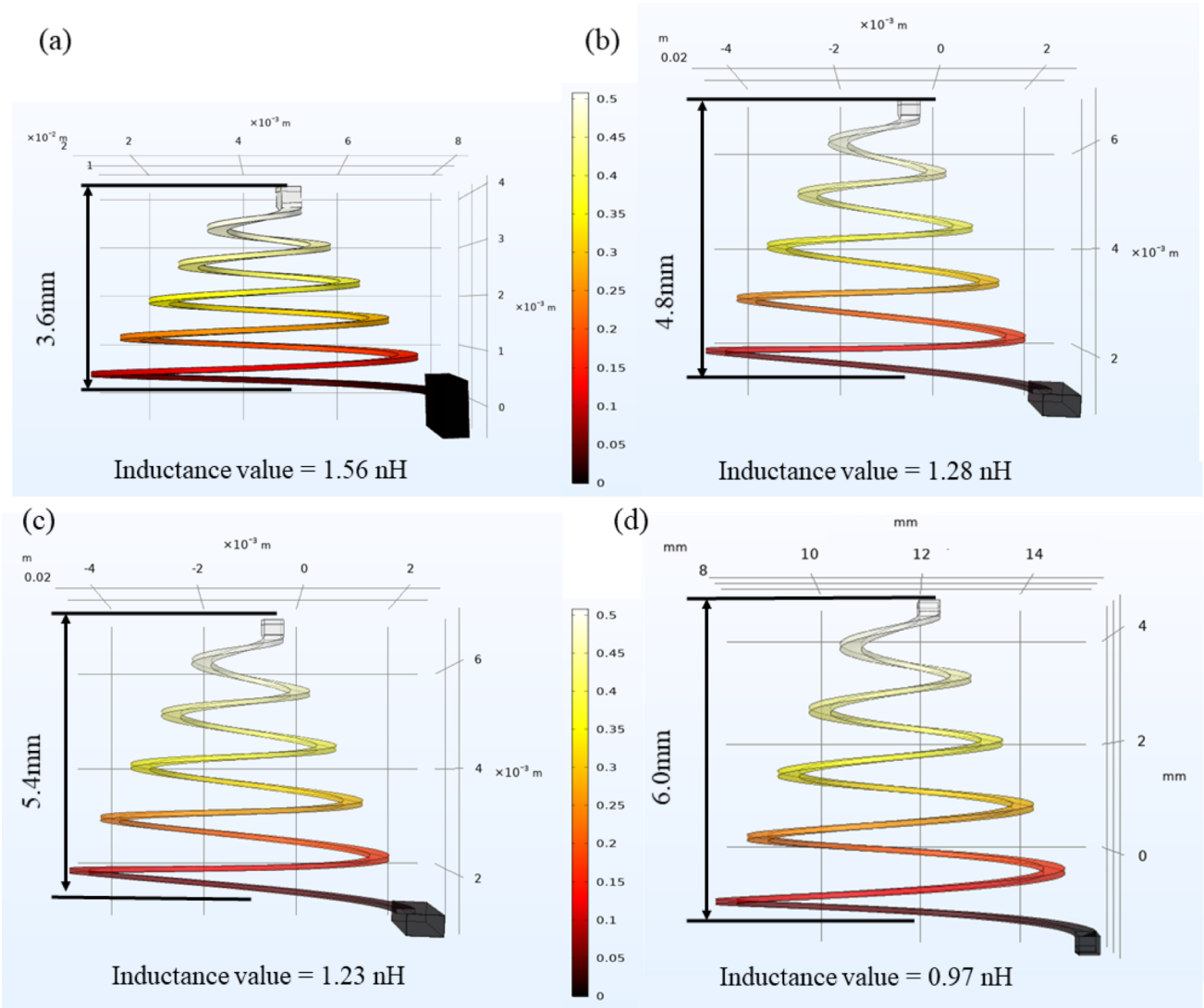

Figure 8. Magnetic and electrical module simulation for different actuation heights of 3D spiral coil inductor. (a)3.6mm actuation (b) 4.8mm actuation (c) 5.4mm actuation (d) 6.0mm actuation

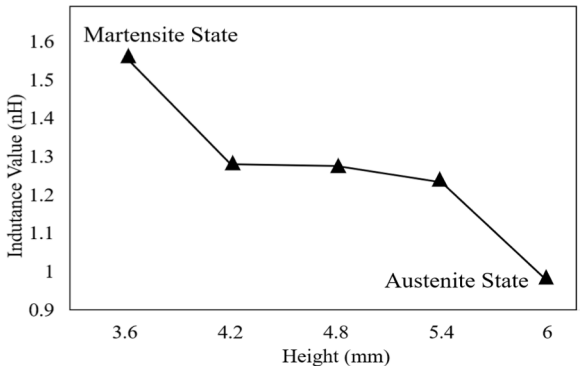

Figure 9: Height (mm) *vs* inductance value (nH)

4. CONCLUSION

A numerical simulation is run for MEMS 3D tunable inductors in both Joule heating module and magnetic and electrical field module. In Joule heating module, the 3D SMA spiral coil is simulated by passing 0.4 A DC current. As stated, that SMA has good electrical conductivity, the heat is evenly distributed between the coils. The inductance value is inversely proportional to the actuation height of the 3D tunable inductor demonstrated in the magnetic and electrical field module. The inductance value is lowest, 0.97nH when the actuation height at its peak, 6mm and highest 1.56nH at 3.6mm. The numerical simulation results will be analyzed and referred before commencing the fabrication and characterization process of the MEMS 3D tunable inductors. This step will simply the future work in developing an ideal MEMS 3D tunable inductor.

ACKNOWLEDGMENT

This work was partially supported by Universiti Teknologi Malaysia under UTMPR Fund (00L28) and Industry-International Incentive Grants (IIIG Q.J130000.3651.03M00 and Q.J130000.3651.03M01).

REFERENCES

[1] Burghartz, J.N. and B. Rejaei, *On the design of RF spiral inductors on silicon.* Electron Devices, IEEE Transactions on, 2003. 50(3): p. 718-729.

[2] Pisani, M.B., et al., *Copper/polyimide fabrication process for above-IC integration of high quality factor inductors.* Microelectronic Engineering, 2004. 73–74(0): p. 474-479.

[3] Hsueh-An, Y., et al. *On-chip high-Q inductor using wafer-level chip-scale package technology*. in *Microsystems, Packaging, Assembly and Circuits Technology, 2007. IMPACT 2007. International*. 2007.

[4] Pirouznia, P. and B.A. Ganji, *Analytical Optimization of High Performance and High Quality Factor Mems Spiral Inductor.* Progress In Electromagnetics Research M, 2014. 34: p. 171-179.

[5] Lakdawala, H., et al., *Micromachined high-Q inductors in a 0.18-μm copper interconnect low-k dielectric CMOS process.* Solid-State Circuits, IEEE Journal of, 2002. 37(3): p. 394-403.

[6] Yue, C.P. and S.S. Wong, *On-chip spiral inductors with patterned ground shields for Si-based RF ICs.* Solid-State Circuits, IEEE Journal of, 1998. 33(5): p. 743-752.

[7] López-Villegas, J.M., et al., *Study of integrated RF passive components performed using CMOS and Si micromachining technologies*. Journal of Micromechanics and Microengineering, 1997. 7(3): p. 162.

[8] Zolfaghari, A., A. Chan, and B. Razavi, *Stacked inductors and transformers in CMOS technology.* Solid-State Circuits, IEEE Journal of, 2001. 36(4): p. 620-628.

[9] Ju-Ho, S., et al. *Multilevel monolithic 3D inductors on silicon*. in *Circuits and Systems, 2001. MWSCAS 2001. Proceedings of the 44th IEEE 2001 Midwest Symposium on*. 2001.

[10] Kim, J.-W., C.-K. Ryu, and Y.-O. Han, *Development of SMD Chip Inductors for RF System Applications*, in *Convergence and Hybrid Information Technology*, G. Lee, et al., Editors. 2012, Springer Berlin Heidelberg. p. 602-610.

[11] Waselikowski, S., et al., *Three-dimensional microcoils as terahertz metamaterial with electric and magnetic response.* Applied Physics Letters, 2010. 97(26): p. 261105.

[12] Young, D.J., et al. *Monolithic high-performance three-dimensional coil inductors for wireless communication applications*. in *Electron Devices Meeting, 1997. IEDM '97. Technical Digest., International*. 1997.

[13] Woytasik, M., et al., *Two- and three-dimensional microcoil fabrication process for three-axis magnetic sensors on flexible substrates.* Sensors and Actuators A: Physical, 2006. 132(1): p. 2-7.

[14] Yonghyun, S., W. Zhengzheng, and M. Rais-Zadeh, *A Multimetal Surface Micromachining Process for Tunable RF MEMS Passives.* Microelectromechanical Systems, Journal of, 2012. 21(4): p. 867-874.

[15] Woytasik, M., et al., *Fabrication of planar and three-dimensional microcoils on flexible substrates.* Microsystem technologies, 2006. 12(10-11): p. 973-978.

[16] Chua, C.L., et al., *Out-of-plane high-Q inductors on low-resistance silicon.* Microelectromechanical Systems, Journal of, 2003. 12(6): p. 989-995.

[17] Zou, J., et al., *Development of three-dimensional inductors using plastic deformation magnetic assembly (PDMA).* Microwave Theory and Techniques, IEEE Transactions on, 2003. 51(4): p. 1067-1075.

[18] Luo, H. and E. Abel, *A comparison of methods for the training of NiTi two-way shape memory alloy.* Smart materials and structures, 2007. 16(6): p. 2543.

[19] Mineta, T., et al., *Batch fabricated flat meandering shape memory alloy actuator for active catheter.* Sensors and Actuators A: Physical, 2001. 88(2): p. 112-120.

[20] Mohamed Ali, M.S., et al., *Radio-Controlled Microactuator Based on Shape-Memory-Alloy Spiral-Coil Inductor.* Microelectromechanical Systems, Journal of, 2013. 22(2): p. 331-338.
[21] Mohan, S.S., et al., *Simple accurate expressions for planar spiral inductances.* IEEE Journal of solid-state circuits, 1999. 34(10): p. 1419-1424.
[22] Guo, Y., et al., *Machinability and surface integrity of Nitinol shape memory alloy.* CIRP Annals, 2013. 62(1): p. 83-86.
[23] AbuZaiter, A., et al., *Design and fabrication of a novel XYθz monolithic micro-positioning stage driven by NiTi shape-memory-alloy actuators.* Smart Materials and Structures, 2016. 25(10): p. 105004.
[24] Hikmat, O., et al. *A monolithic tunable out-of-plane inductor based on NiTi two-way shape-memory-alloy*. in *2017 19th International Conference on Solid-State Sensors, Actuators and Microsystems (TRANSDUCERS)*. 2017. IEEE.